ELSEVIER

Journal of Materials Processing Technology 94 (1999) 133–140

Journal of Materials Processing Technology

www.elsevier.com/locate/jmatprotec

# A comparative evaluation of gas tungsten and shielded metal arc welds of a ‘‘ferritic’’ stainless steel

T. Mohandas[a,*], G. Madhusudhan Reddy[a], Mohammad Naveed[b]

[a]*Defence Metallurgical Research Laboratory (DMRL), Kanchanbagh, Hyderabad 500 058, India*
[b]*Regional Engineering College, Warangal, India*

Received 9 February 1998

**Abstract**

The effect of welding process shielding gas and the addition of grain refining elements on the weld zone tensile properties of a ferritic stainless steel conforming to AISI 430 has been investigated. Gas tungsten arc welds exhibiting equi-axed grain morphology had superior tensile and yield strength compared to shielded metal arc welds. The tensile ductility of gas tungsten arc welds was also on an average marginally greater than that of shielded metal arc welds. Welds in general showed low ductility compared to that of the base metal. The addition of titanium and copper led to improved strength over that of the base alloy. The observed properties could be correlated to the austenite content and the fracture morphology. © 1999 Elsevier Science S.A. All rights reserved.

*Keywords:* Gas tungsten arc; Shielded metal arc; Ferritic stainless steel

## 1. Introduction

Ferritic stainless steels are used commonly due to their corrosion resistance at room temperature. They are a cheaper alternative to austenitic stainless steels. In such applications as the production of titanium by Krolls process, where titanium tetrachloride is reduced by magnesium, austenitic stainless steels are used for the reduction retorts with an inner lining of ferritic stainless steels to mitigate the problem of leaching of the nickel by molten magnesium. In the fabrication of these structures, welding is employed extensively. The present study is related to the gas tungsten welding aspects of 17 Cr ferritic stainless steel, equivalent to AISI 430. The heat of welding leads to grain coarsening in the heat-affected zone and in the weld metal of ferritic stainless steels because they solidify directly from the liquid to the ferrite phase without any intermediate phase transformation. It is therefore recommended that these alloys are welded with a low heat input and at high welding speeds [1]. Attempts have been made to grain refine the welds of these steels by the addition of elements such as Ti and Al [1]. Studies have also been conducted to grain refine ferritic stainless steel welds by electromagnetic stirring [2] as well as through liquid metal chilling [3]. The effect of these grain-refining techniques on mechanical properties has not hitherto been reported. In duplex stainless steels the addition of copper to the weld pool is also reported to lead to microstructural refinement due to the pinning effect of copper particles at the austenite grain boundaries and due to the formation of fine, homogeneously distributed, twinned austenite needles [4].

For thin sections, gas tungsten arc welding with inert gas shielding by argon, helium or a mixture of the two, and for thick sections, gas metal arc welding has been reported to be favourable (5). The addition of oxygen in the shielding gas mixture has also been reported to prevent arc wander and nitrogen pick-up in the weld [5]. In general, the ductility of ferritic stainless steel welds is reported to be low due to large grain size of the fusion zone [6,7].

Keeping this in mind, the present study aimed at investigating the influence of grain refiners, gas shielding, as well as the welding process, on the tensile properties of the weld zone of a ferritic stainless steel conforming to AISI 430 with the nominal composition as given in Table 1. Two welding processes, namely, gas tungsten arc welding (GTAW) and shielded metal arc welding (SMAW), were employed in the study. The effects of adding oxygen in the shielding gas, grain refiner (Ti) and austenite stabilizer (copper) were also investigated.

*Corresponding author. Tel.: +91-40-444-0051; fax: +91-40-444-0683.


PII: S0924-0136(99)00092-8

Table 1
Nominal compositions of the base alloy and the all-weld of SMAW and GTAW

| Material | Element (wt%) | | | | | | |
|---|---|---|---|---|---|---|---|
| | C | Mn | Si | Ni | Cr | S | P |
| Base alloy | 0.06 | 0.4 | 0.55 | 0.19 | 17.0 | 0.005 | 0.052 |
| SMAW all-weld | 0.1 | 1.0 | 0.9 | 0.6 | 17.0 | 0.03 | 0.04 |
| GTAW all-weld | 0.1 | 0.8 | 1.0 | 0.6 | 17.0 | 0.03 | 0.04 |

Table 2
Details of welding process variables

| Parameters | GTAW | SMAW |
|---|---|---|
| Electrode diameter (mm) | 1.6 | 4.0 |
| Welding speed (mm/min) | 50 | 200 |
| Arc voltage (V) | 18 | 18–20 |
| Welding current (A) | 100 | 100 |
| Arc gap (mm) | 2 | 2 |
| Gas flow rate ($m^3$/h) | 0.57 | – |

## 2. Experimental

### 2.1. Welding

Cold rolled sheet of AISI 430 steel of 3 mm thickness was used with the microstructure shown in Fig. 1. The microstructure consists of an elongated morphology of ferrite due to the rolling texture inherited from the cold rolling operation. A square butt-joint configuration (Fig. 2) was selected. During shielded metal arc welding the coated electrodes gave the all-weld metal composition shown in Table 1. For GTAW, a filler wire conforming to the composition given in Table 1 was used. Titanium was added as a powder obtained from crushed titanium sponge and copper was added as a foil between the butt joint. Oxygen was added as a 2% $O_2$+98% Ar mixture. The welding conditions are given in Table 2.

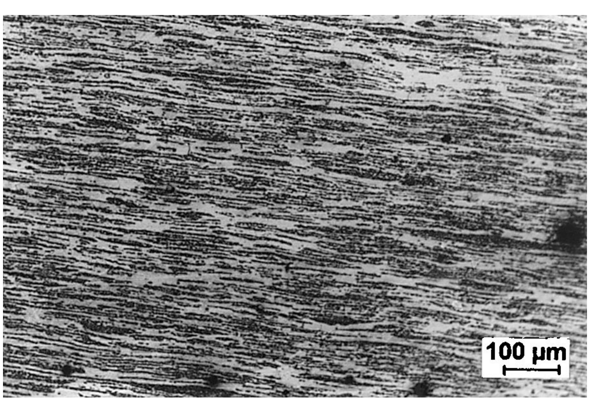


Fig. 1. Microstructure of the base metal.

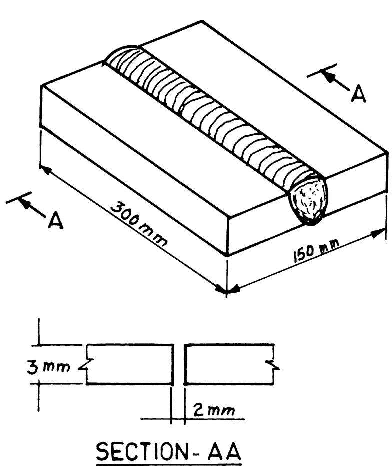


Fig. 2. Configuration of the weld joint.

### 2.2. Metallography

Conventional optical microscopy was employed for microstructural studies. An ISI 100 scanning electron microscope was used for fractographic examination. An AST 2000 X-ray stress analyser with a provision to determine austenite was utilised for the measurement of austenite content using Cr $K_\alpha$ radiation with point source of X-rays. The measurements are based on the (2 1 1) austenitic peak.

### 2.3. Mechanical properties

Fusion-zone tensile properties were evaluated on an Instron 1100 test system. The configuration of the tensile specimen adopted is given in Fig. 3. The specimen configuration was so selected that fracture occurred in the weld region only. The hardness in the weld region was measured using a Vickers Pyamid micro-hardness tester.

## 3. Results

### 3.1. Metallography

The macro- and micro-structures are presented according to the welding process (Figs. 4 and 5), the effect of oxygen (Figs. 6 and 7) and the effect of copper and titanium addition (Figs. 8 and 9). The micro-structure of SMAW weld consisted of predominantly columnar fusion zone grains, whilst the fusion-zone grain structure in GTAW was equi-axed. The growth direction of grains in SMAW was from the face side to the root side suggesting minimum heat flow in the lateral direction. The pattern of grain growth in the two welding processes did not change with the addition of argon, copper or titanium, however, their addition did decrease the size of the fusion-zone grains, this tendency being more pronounced for the copper addition (Table 3).

The austenite content in the weld region is listed in Table 4. In general, the shielded metal arc welds contained more austenite. This could be due to nitrogen pick-up from the atmosphere in respect of SMAW. Nitrogen is a well-known austenitic stabilizer. The greatest amount of austenite (67%) was found when copper was added in the SMAW

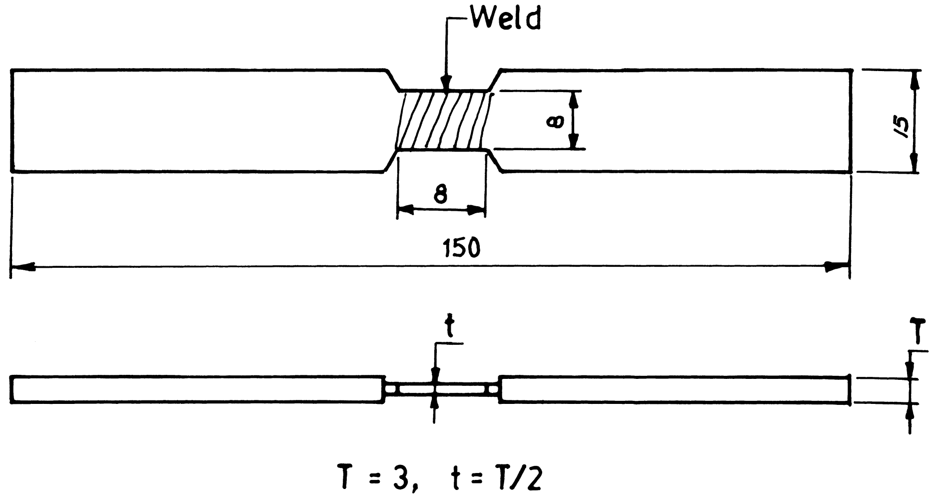


Fig. 3. Geometry of the tensile specimens (dimensions: mm).

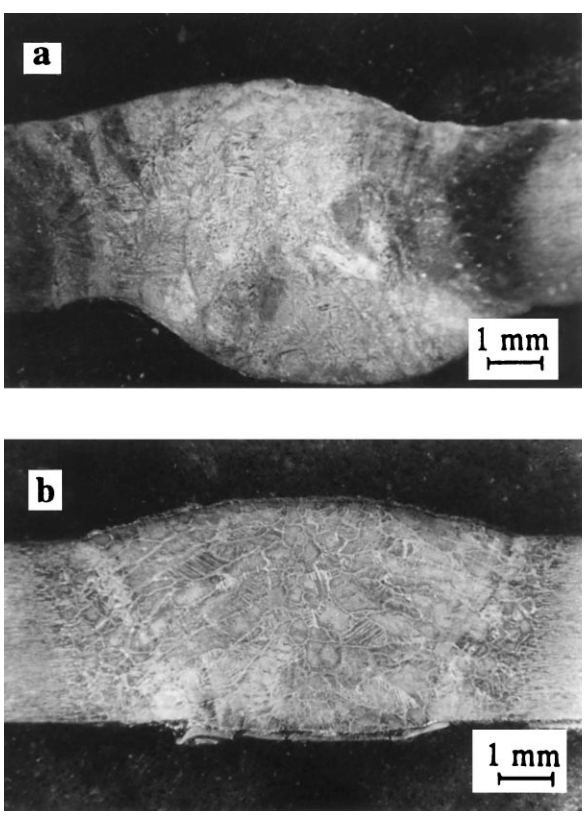


Fig. 4. The macrostructure of: (a) an SMAW weld; (b) a GTAW weld.

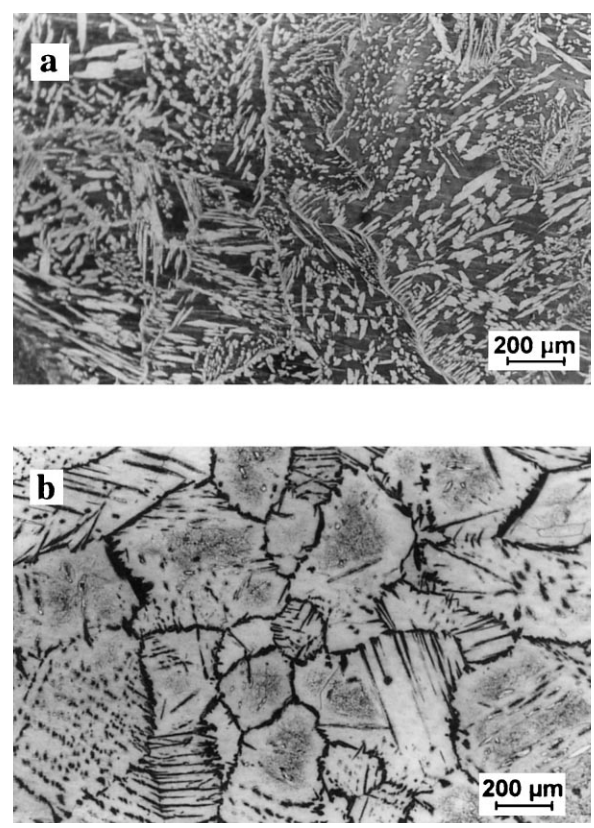


Fig. 5. The microstructure of: (a) an SMAW weld; (b) a GTAW weld.

Table 3
Data on the fusion-zone grain size and the morphology of the grains

| Condition | SMAW | | GTAW | |
|---|---|---|---|---|
| | Grain size (μm) | Grain morphlogy | Grain size (μm) | Grain morphlogy |
| Normal | 600 | Columnar | 350 | Equi-axed |
| Ar+2% $O_2$ | 300 | Columnar | 100 | Equi-axed |
| Cu addition | 200 | Columnar | 150 | Equi-axed |
| Ti addition | – | – | 200 | Equi-axed |

Width of the grains is taken as grain size in respect of columnar grains.

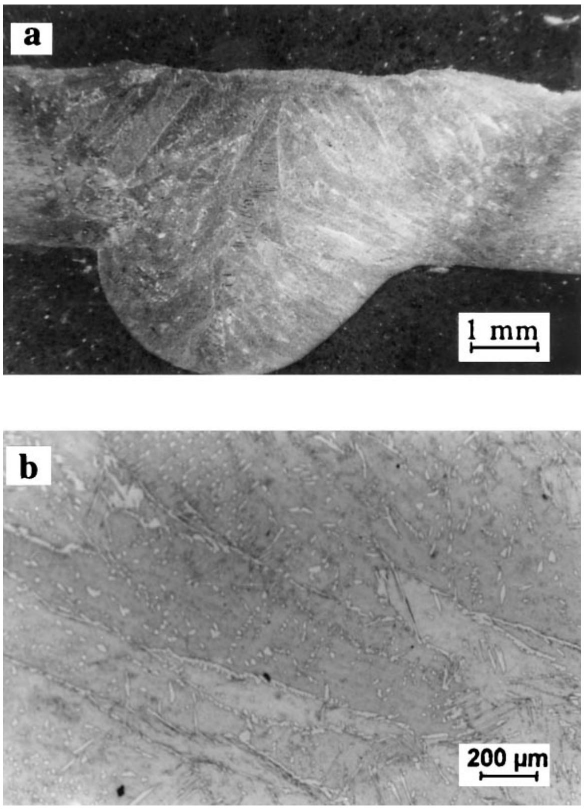


Fig. 6. The effect of oxygen on the SMAW weld zone: (a) macrostructure; (b) microstructure.

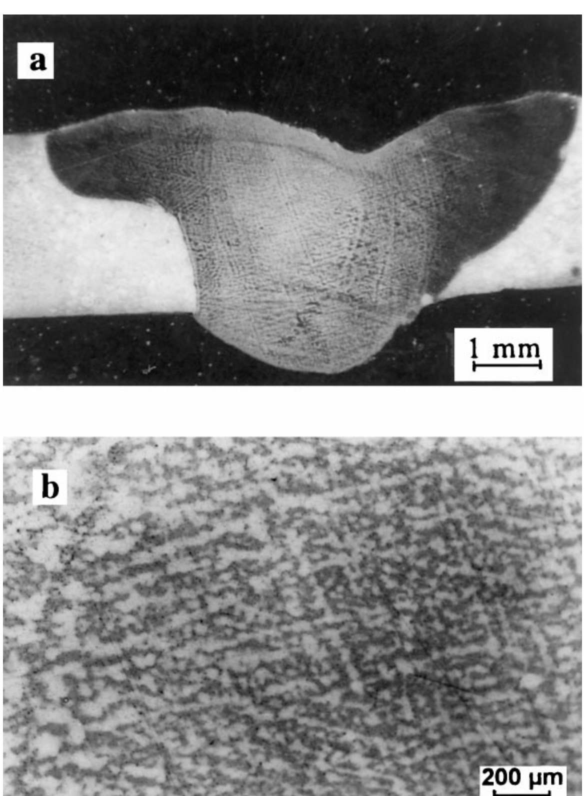


Fig. 7. The effect of oxygen on the GTAW weld zone: (a) macrostructure; (b) microstructure.

Table 4
Data on retained austenite content of welds

| Austenite (%) | | |
|---|---|---|
| Condition | GTAW | SMAW |
| Normal | 4.5–6 | 9–12 |
| Argon+2% $O_2$ shielding | 9–12 | 14–17[a] |
| Ti addition | 12–15 | – |
| Cu addition | 15–17 | 64–68 |

[a] Back purged with Ar+2% $O_2$.

process, whilst the lowest value (5%) was present in the normal GTAW. Back purging with Ar+2% $O_2$ in the SMAW resulted in the increase in the austenite content, which could be due to the combination of chromium with oxygen. This could lead to the non-availability of chromium to such an extent so as to affect ferrite stabilization. The addition of Ti as well as Cu led to an increase in the austenite content. The increase in austenite content when copper is added can be attributed to the austenite stabilizing effect of coper [4]. The role of titanium in increasing the austenite content is intriguing. Titanium is known to be a ferrite stabilizer [8]. It is also known that titanium in maraging steels is reported to lead to more retained austenite in the welds [9], in present day maraging steels titanium being partially replaced by aluminium.

### 3.2. Mechanical properties

Hardness data of the fusion zone of the weldments are listed in Table 5. On an average, the hardness of the GTAW welds was lower than that of the SMAW welds. In shielded metal arc welding, argon+2% $O_2$ backing as well as the addition of copper resulted in decreased hardness. The addition of copper led to the maximum reduction in hardness. In gas tungsten arc welding, the addition of oxygen in the shielding gas and titanium addition led to a reduction in hardness, whilst the addition of copper increased the hardness. In general, the hardness reduced as austenite content increased, an exception being the copper-added gas tungsten arc weld (Fig. 10). This could be due to the precipitation hardening effect of copper.

The tensile properties of the weld zone of shielded metal arc and gas tungsten arc welds are presented in Tables 6 and 7, respectively. In general, the strength and ductility of gas tungsten arc welds were greater. The addition of oxygen in

Table 5
Micro hardness ($H_v$) of the fusion zone of the weldments

| Condition | SMAW | GTAW |
|---|---|---|
| Normal | 305 | 210 |
| Argon+$O_2$ | 247 | 166 |
| Cu addition | 184 | 290 |
| Ti addition | – | 166 |

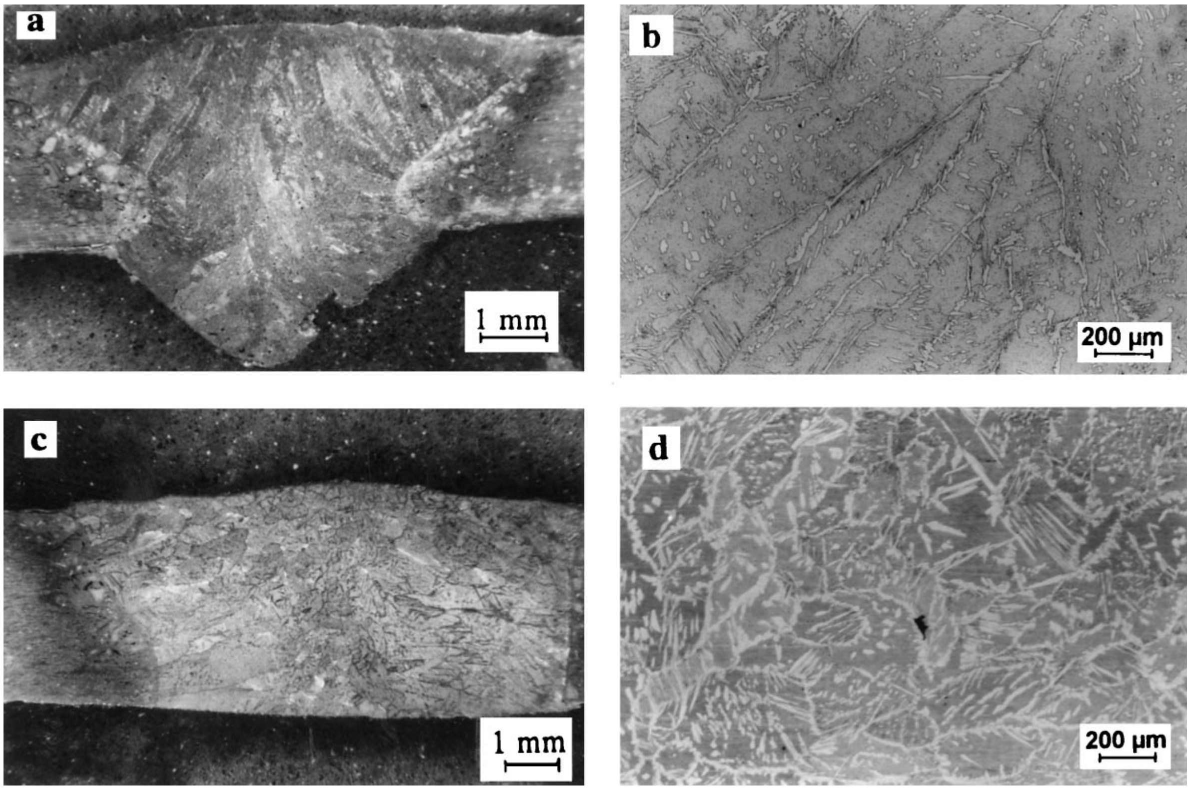


Fig. 8. The effect of copper addition on the weld-zone microstructure: (a, b) SMAW; (c, d) GTAW.

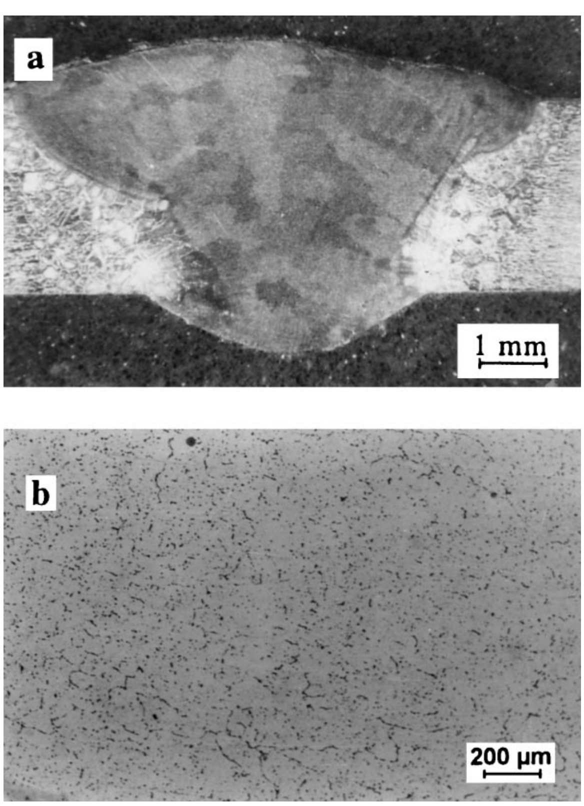


Fig. 9. The effect of titanium on the GTAW weld-zone: (a) macro-structure; (b) microstructure.

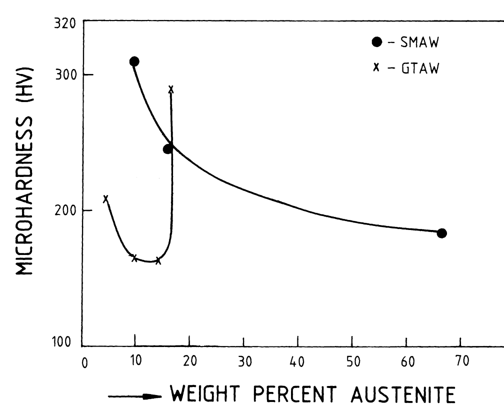


Fig. 10. The influence of the austenite content on the weld-zone hardness.

Table 6
Weld-zone tensile properties of SMAW

| Condition | 0.2% YS (MPa) | TS (MPa) | El (%) | Austenite (wt%) |
|---|---|---|---|---|
| Normal | 217 | 605 | 6.7 | 9–12 |
| Argon+2% $O_2$ back purging | 219 | 498 | 4.1 | 14–17 |
| Cu addition | 429 | 841 | 5.1 | 64–68 |
| Base metal | 330 | 745 | 11.0 | – |

Table 7
Weld-zone tensile properties of GTAW

| Condition | 0.2% YS (MPa) | TS (MPa) | El (%) | Austenite content (wt%) |
|---|---|---|---|---|
| Argon shielding | 365 | 600 | 7.8 | 4.5–6 |
| Argon+2% $O_2$ shielding | 304 | 516 | 5.0 | 9–12 |
| Ti addition | 384 | 562 | 4.0 | 12–15 |
| Cu addition | 426 | 979 | 6.6 | 15–17 |

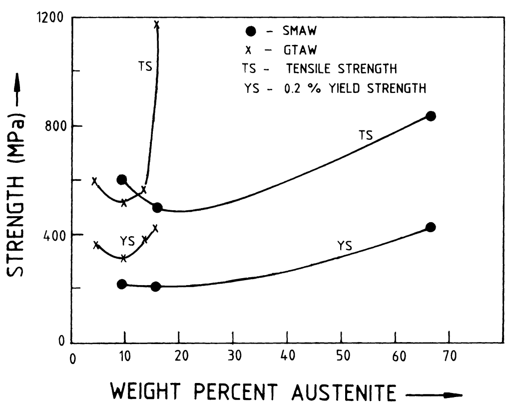


Fig. 11. The effect of the austenite content on the strength of the weld zone.

the shielding gas in GTAW and Ar+$O_2$ backing in SMAW reduced the ductility as well as the strength. The addition of copper led to an increase in strength and a reduction in ductility. The addition of titanium in the gas tungsten arc weld showed a similar effect as that of copper on ductility. However, the reduction in ductility was maximum in the case of titanium addition. The strength improvement was substantial with copper addition, with marginal reduction in ductility compared to that of normal welding. The variation of the yield and tensile strength with the austenite content of the weld zone is presented in Fig. 11. It is to be noted that initially the strength decreases with increase in the austenite content, whilst further increase in the austenite content results in increased strength. This could be due to the precipitation-hardening effect of copper, which becomes prominent only at high austenite content, leading to a possible change in the fracture mechanism.

### 3.3. Fractography

The effect of the welding process on the fractographic features is shown in Fig. 12. The fracture is predominantly by cleavage. The average facet size at the macro level is smaller for GTAW. At higher magnification, a greater degree of ductile features is evident in GTAW. The average facet size increased with oxygen addition to the shielding gas in GTAW, and back purging with Ar+2% $O_2$ in SMAW

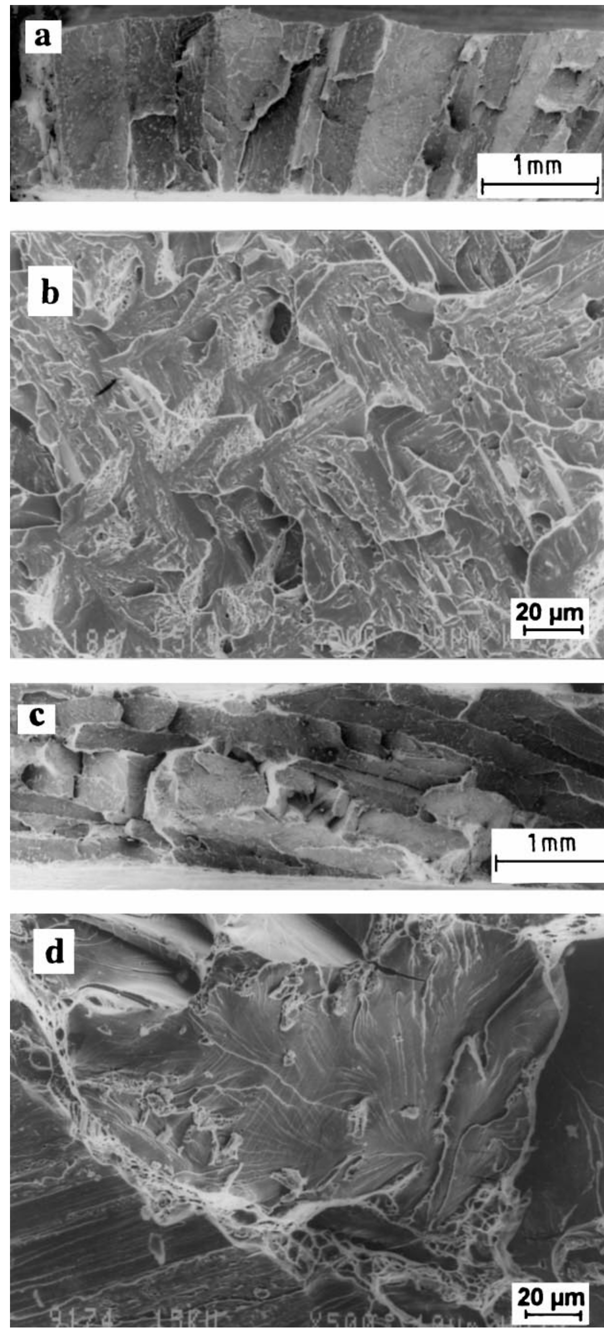


Fig. 12. The effect of the welding process on the fractographic features: (a, b) SMAW; (c, d) GTAW.

(Fig. 13). Copper addition to the weld pool decreased the facet size in SMAW, the facets being predominantly equi-axed (Fig. 14) when compared to the fractographs of welds without copper addition. The addition of Cu (Fig. 14(c) and (d)) as well as Ti (Fig. 15) to the weld pool decreased the facet size in GTA welds. Copper addition has a greater influence, in that the facets are more equi-axed. This observation suggests that copper addition is more beneficial than titanium addition in altering the grain structure of the fusion zone to equi-axed morphology.

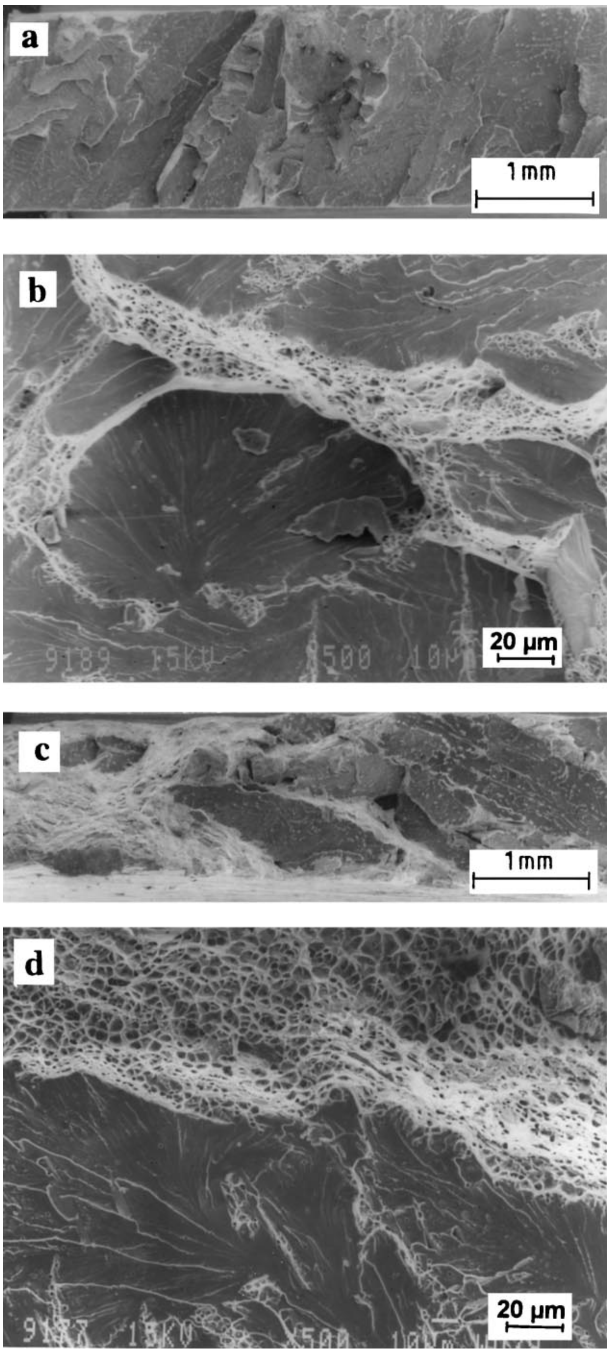


Fig. 13. The effect of oxygen on the fractographic features: (a, b) SMAW; (c, d) GTAW.

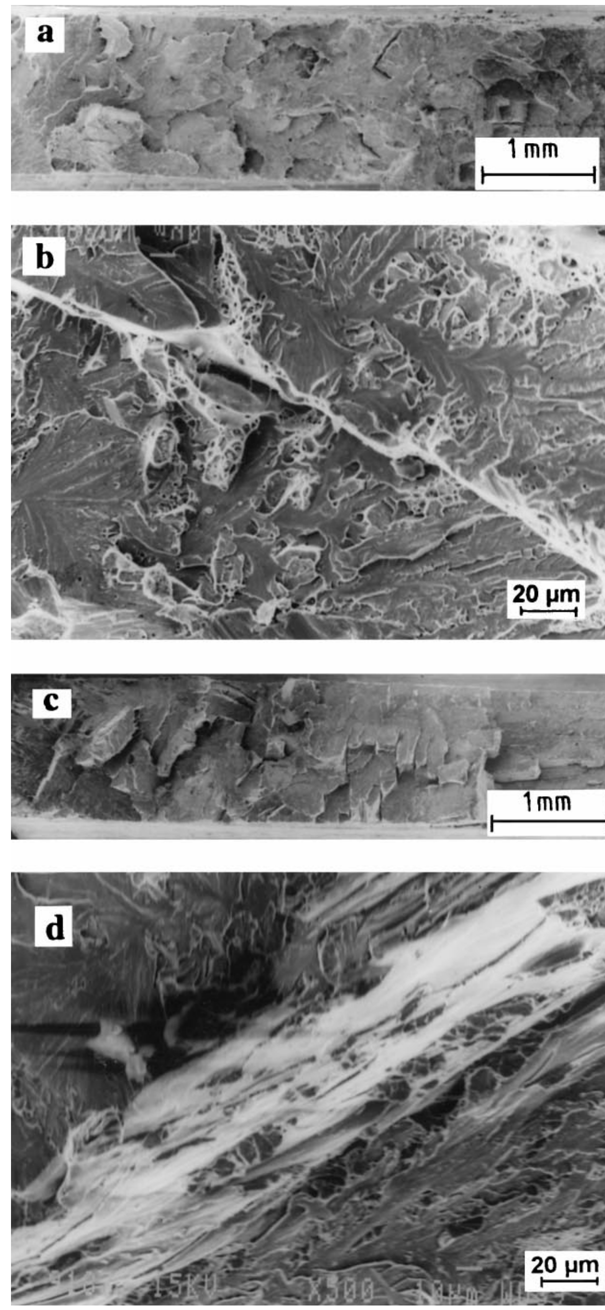


Fig. 14. The effect of copper on the fractographic features: (a, b) SMAW; (c, d) GTAW.

## 4. Discussion

The greater ductility and strength of gas tungsten arc welds as compared to those of shielded metal arc welds can be attributed to the equi-axed morphology of the fusion-zone grains in the gas tungsten arc welds, and also to inert gas shielding. The general low ductility of welds compared to that of the initial base metal can be due to the cast microstructure of the fusion zone [10]. Decreased ductility and strength when oxygen is added can be attributed to the vertical growth of grains in SMAW and the loading being perpendicular to the long axis of the fusion-zone grains along which the strength and ductility are expected to be low.

The addition of titanium to the GTAW weld pool, which has resulted in decreased tensile strength and a marginal decrease in ductility, is in conformity with the trends that titanium additions beyond 0.17 wt% to ferritic stainless steel results in decreased ductility and fracture stress [11]. However, the observed increase in the yield strength is not

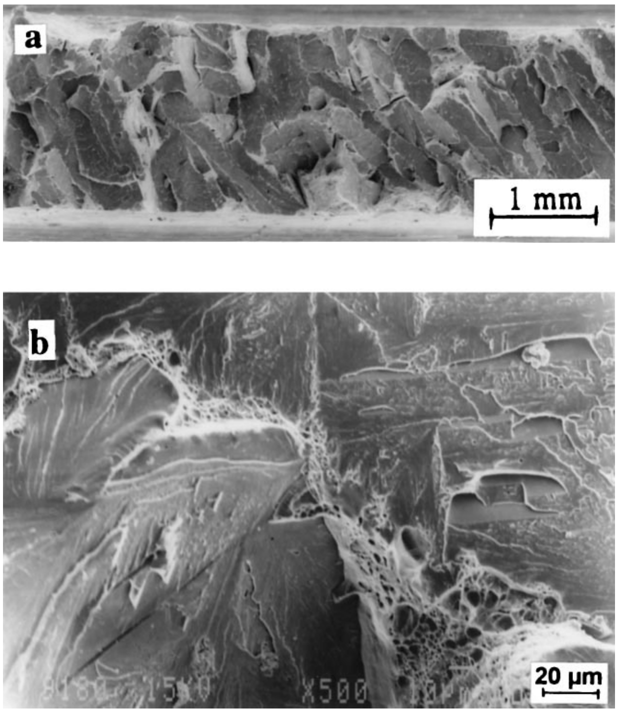

Fig. 15. The effect of tianium on the fractographic features.

explainable, as the yield stress is also supposed to decrease [11]. The yield strength increase can only be attributed to solid-solution strengthening and strengthening by the formation of titanium carbonitrides that are believed to be responsible for grain refinement [1]. As titanium addition is not in a controlled percentage, the titanium added can be in excess of that required for the formation of TiC and Ti(CN) and hence can contribute to solid-solution strengthening. The trends observed with copper addition are well reflected in the facet size as well as in the strength. The role of Cu addition is similar to that reported in respect of duplex stainless steels (4) and is substantiated by the highest proportion of austenite content when copper is added to the weld zone. A general trend is that in each welding process the strength increased with increase in the austenite. The highest strength of welds with copper addition can be attributed to a combination of grain refinement as well as precipitation strengthening by copper precipitates.

The contradictory trends observed in respect of hardness and strength are not understood at this juncture. It may however be viewed that strength is derived through the grain-boundary strengthening effect of precipitate at the grain boundaries and that this effect would not be reflected in hardness, as the latter does not give a global picture, whilst strength reflects a global picture. This view is supported by the additions of titanium, zirconium or columbium being reported to reduce yield strength and increase fracture stress [11].

The use of a protective gas shielding in gas tungsten arc welding and the addition of grain refiners such as Cu and Ti did improve the strength and decrease the facet size. However, the ductility values remained low. These trends can only be attributed to a presumably greater level of interstitials, namely C and N. The predominantly cleavage-fracture features support this view. A post-weld ameal at 820°C followed by a water quench, which has been reported to increase ductility [11], might offer a solution.

## 5. Conclusions

1. Gas tungsten arc welds exhibited greater strength as well as ductility presumably due to the equi-axed fusion zone grain morphology and the protective nature of the shielding gas, which can shield the weld pool from the entry of nitrogen from the atmosphere.
2. Copper addition resulted in substantial improvement in strength without adversely affecting the ductility. This can be attributed to the highest percentage of retained austenite and a grain-refinement action by the copper precipitates, as is reported in respect of duplex stainless steels.
3. In each welding process the strength improved as the retained austenite content increased.

## Acknowledgements

The authors are thankful to Dr. D. Banerjee, Director, and Dr. C.R. Chakravorthy, Associate Director, of the Defence Metallurgical Research Laboratory for their continued support and encouragement.

## References

[1] J.C. Villafuerte, E. Pardo, H.W. Kerr, Metall. Trans. A 21A (1990) 2009–2019.
[2] J.C. Villafuerte, H.W. Kerr, Weld. J. 69 (1990) 1s–13s.
[3] J.C. Villafuerte, H.W. Kerr, S.A. David, Mater. Sci. Eng. A 194 (1995) 187–191.
[4] B. Soylu, R.W.K. Honeycombe, Mater. Sci. Eng. A 7 (1991) 137–144.
[5] K.E. Dorschu, Weld. J. 50 (1971) 408s–418s.
[6] J.C. Hedge, Metal Prog. 27(4) (1935) 33–38.
[7] W.B. Miller, Metal Prog. 20(12) (1931) 68–72.
[8] F.B. Pickering, Int. Met. Rev. (1976) 227–268.
[9] N. Kenyon, Weld. J. 47 (1968) 193s–198s.
[10] L.K. Stringham, The Iron Age 160 (1947) 61–63.
[11] B. Pollard, Welding. J. 51 (1972) 222s–230s.